Hindawi
Advances in Civil Engineering
Volume 2021, Article ID 4960461, 10 pages
https://doi.org/10.1155/2021/4960461

Research Article

Study on the Comfort of Pedestrians on Landscape Footpath Paved on the Suspension Monorail System

Zhou Li,[1] **Yuancheng Wei**,[2] **Xiaolong Zheng**,[3] **Yongping Zeng**,[3] **Xinyu Xu**,[3] **Xingyu Chen**,[3] **and Qi Tao**[3]

[1]*China Construction Science and Industry Corp. Ltd., Shenzhen 518048, Guangdong, China*
[2]*Construction Affairs Bureau of Shenzhen Longhua District (Rail Transit Construction Management Center of Shenzhen Longhua District), Shenzhen 518028, Guangdong, China*
[3]*China Railway Eryuan Engineering Group Co., Ltd., Chengdu 610031, Sichuan, China*

Correspondence should be addressed to Zhou Li; 976112542@qq.com

Received 8 November 2021; Accepted 13 November 2021; Published 27 November 2021

Academic Editor: Ping Xiang

This is the first time that the landscape footpath is realized on the suspension monorail system. To study the comfort of pedestrians on the landscape footpath when the vehicle passes, the dynamic responses of the track beam and the landscape footpath at different speeds were analyzed using the established vehicle-bridge dynamic analysis model. To evaluate the comfort of pedestrians on the landscape footpath, two indexes, Root Mean Square (RMS) value of acceleration (ISO 10137) and peak value of acceleration (EN 03), were adopted. Results show that the displacement and acceleration responses of landscape footpath and track beam are obviously different. Vertical displacement of the track beam is much larger than that of the landscape footpath due to the eccentric load of vehicles. Due to the displacement and rotation of the structural components which support the landscape footpath, the lateral response transferred to the landscape footpath would be slightly weakened. Maximum RMS values of the lateral and vertical acceleration of landscape footpath are 0.162 m/s^2 and 0.169 m/s^2, respectively, which meet the requirements of ISO 10137. Peak lateral acceleration is 0.546 m/s^2, which reaches CL3 standard, and the peak vertical acceleration is 0.548 m/s^2, which reaches CL2 standard. Lateral comfort is slightly worse than vertical comfort.

1. Introduction

Monorail transit system regards the strip beam as the pathway, where the vehicles ride on the beam or are suspended under the beam. The first suspension monorail system was built in Wuppertal in Germany along the river in 1901. Recently, the suspension monorail has been discussed as an effective transportation solution for connecting different urban areas or scenic areas. Under this circumstance, the landscape footpath has been proposed to integrate with one of the commercial-operated suspension monorails in a tourist attraction in China, to improve the tourists' experience, and to optimize the structural dynamic performance of the vehicle. It is the first case to add a landscape footpath on the track beam. Due to the large width-span ratio of the design, the proportion of the live load and dead load of the monorail system is much larger than that of the conventional wheel-rail system. Meanwhile, for the steel structure design of the monorail, the structural damping is small. Relative standards in China, "Code for Design of Urban Rail Transit Bridge" GB/T 51234-2017 [1] and "Technical Standard for Suspension Monorail Transit" DBJ41/T217-2019 [2], have no clear requirements for the dynamic responses of the monorail bridge style. Therefore, the influence of the bridge vibration induced by the passing vehicles on the comfort of pedestrians on the footpath becomes a practical issue that needs to be explored.

With the rapid development of suspension monorail transit system in recent years, several researches on the dynamic characteristics of the system have been conducted. Bao et al. [3, 4] utilized the cosimulation method to study analysis responses of monorail vehicle and bridge, in which

the effects of tyre stiffness, crosswind, and operating condition were discussed. He et al. [5] carried out field measurement on dynamic responses of suspension monorail system for straight and curved line. Taking the curved monorail bridge as research project, Yang et al. [6] took nonlinear radial stiffness of a suspension monorail rubber tyre into consideration and analyzed several key parameters. Zou et al. [7] investigated the aerodynamic characteristics and interference effects for different spacing ratios (line distance to beam width) of track beam via wind tunnel test and CFD (Computational Fluid Dynamics) simulation.

Traditional research on the comfort of pedestrians commonly focused on pedestrian bridges. Most related works discussed the dynamic responses of bridges under the actions of pedestrians. Feng et al. [8] carried out the actual measurement and questionnaire of pedestrians on 21 footbridges, obtained a comfort design curve of pedestrian bridge based on peak acceleration, and proposed a comfort design method of pedestrian bridge. Based on the principle of probability and statistics, Chen et al. [9] combined the human body resistance and vibration effect and proposed a mathematical definition of sensitivity. Ma et al. [10] conducted an experiment to study the perception of human-induced vibrations of footbridges and proposed perception scales for lateral and vertical vibrations of footbridges. Bhowmik et al. [11] utilized an image processing technique and an automated enhanced frequency-domain decomposition technique to evaluate the damping of the suspension footbridge with 1.37 m width. Apart from the pedestrian loads, the pedestrian bridge integrated in the complex traffic system may receive other external excitations, which might have impacts on the pedestrian comfort level. Responses of the pedestrian bridge under vehicle-induced excitation were analyzed by some researchers, and the effects of the roughness of road surface, vehicle speed, and traffic flow on the responses were discussed as well [12, 13].

The article takes the aforementioned 5-span 40 m simply supported suspension monorail system with landscape footpath project as an example, and the dynamic characteristics of the monorail system with the monorail vehicle passing at operating speed are analyzed. The comfort of pedestrians on the landscape footpaths at different vehicle speeds is evaluated based on the criteria of pedestrian comfort. The results provide a helpful and reasonable reference for the future design. Section 2 presents the established vehicle-bridge coupled model for the dynamic analysis of the suspension monorail system, including the vehicle model, bridge model, and tyre model, as well as the dynamics of multibody system used in the model. Section 3 illustrates the two criteria for the comfort of pedestrians on the landscape footpath. The dynamic responses of both landscape footpath and track beam are analyzed and the comfort of pedestrians on the footpath is evaluated in Section 4. Finally, the conclusions are given in Section 5.

2. Vehicle-Bridge Coupled Model

The vehicle-bridge coupled model is a combined system composed of vehicle and bridge models on the basis of the wheel-rail motion relationship [14–17]. Unlike the traditional wheel-rail contact method, the contact method in the suspension monorail needs to take the tyre model into consideration, due to the fact that the tyre of vehicle is in contact with the beam [18–20].

In the paper, the multibody dynamic software SIMPACK and finite element software ANSYS were used to establish the monorail vehicle and bridge models, respectively. The information of bridge, including structure information (stiffness and mass information), model information, and geometry information, was obtained by substructure analysis in the finite element software. Then, the information of bridge was introduced into the multibody dynamic software via interface program, the bridge was modelled as the flexible body, and the dynamic coupled model was analyzed in multibody dynamic system.

2.1. Flexible Body in Multibody Dynamics. In the multibody system, the bridge structure is regarded as a flexible body [21, 22]. The position of point P on the flexible body can be expressed as

$$r^P(c,t) = A(t)(r + c + u(c,t)), \tag{1}$$

where A is the rotation matrix from the reference coordinate system to the inertial coordinate system of the body; r is the position in the reference coordinate system; c is the position of point P in the reference coordinate system under the nondeformation state; and $u(c,t)$ is the deformation vector of the flexible body.

The Ritz of the deformation of the flexible body can be approximated via the linear combination of the shape function $\phi_j(c)$ and the mode coordinate $q_j(t)$ as

$$u(c,t) = \sum_{j=1}^{n_q} \phi_j(c) q_j(t). \tag{2}$$

Based on the Ritz approximation and Hamilton principle, the motion equation can be expressed by the variational method as

$$M(q)\begin{Bmatrix} a \\ \dot{\omega} \\ \ddot{q} \end{Bmatrix} + k\omega(\omega, q, \dot{q}) + k(q, \dot{q}) = h, \tag{3}$$

where M is the mass matrix; k_ω is the generalized force matrix of the rotational and centrifugal items; k and h are the generalized force matrices of the internal force and external force, respectively; a, ω, and q are the absolute acceleration, angle acceleration, and modal coordinate, respectively.

2.2. Monorail Vehicle Model. The single vehicle of suspension monorail is composed of a car body and two bogies. The car body and bogie are connected by suspension devices, dampers, bolsters, and pins. The whole bogie is arranged in the C-beam body. The stiffness of the traveling tyre is defined as 13.3×10^6 N/m, which is provided by the vehicle manufacturer. The guide wheels on both sides of the bogies are

constrained by the beam webs to realize the steering function. Both the car body and frame include 5 degrees of freedom, which are lateral, vertical, yaw, pitch, and roll motions. Therefore, a single vehicle has 31 degrees of freedom in total.

In the numerical simulation, the car body and frame are regarded as rigid bodies, and the suspension and dampers are regarded as force elements. The scheme of the single vehicle model is shown in Figure 1. The monorail train applies three-vehicle marshalling, and the speeds are 20, 30, 40, 50, and 60 km/h. The load of each axle (at full capacity) is 5.5 tons.

2.3. Bridge Model. The paper employs a 5×40 m simply supported bridge. The single track beam is in the form of a thin-walled C-shaped steel box girder with an opening in the bottom. The beam height is 1.31 m at the track beam end and 2.07 m in the midspan, and it linearly increases from 1.31 m (3 m from the beam end) to 2.07 m (9 m from the beam end). The inner width of the track beam is 0.78 m, and the cross section of the beam end is shown in Figure 2. The double-track monorail track beams are all placed underneath the cover beam of the pier. The distance between the double-track lines is 5.1 m, and the width of the landscape footpath on the beam is 7.2 m. The steel pier is 16 m in height, 1.34 m in width in the longitudinal direction, and 0.9 m in the transverse direction, whose cross section is a closed rectangular cross section. The inner width of track beam is 0.78m, and the cross section of the beam end is shown in Figure 2.

The bridge model was established in the commercial finite element software ANSYS. The plate element is applied to the track beam and landscape footpath in the model, and the spatial beam element is exerted to the pier. The elastic modulus and Poisson's ratio of components are taken in accordance with the relevant design standards. The secondary dead load is evenly added to the beam elements uniformly. The finite element model has 29409 nodes and 30261 elements in total. The bridge model is shown in Figure 3. The damping ratio of the bridge is considered as 0.5%.

Natural frequency analysis of the bridge model is performed, and the typical frequencies and corresponding mode shape descriptions are shown in Table 1 and Figure 4. It can be seen from the results that the frequencies of the pier are relatively low and flexible, and the frequencies of the track beam are above 3 Hz. However, due to the small ratio of the dead load and live load on the suspension monorail beam, the dynamic responses of the bridge under the live load of the vehicle would be probably significant.

2.4. Tyre Model. Suspension monorail system adopts the rubber tyre for the link of the vehicle and track beam. The rubber traveling wheels of the vehicle directly act on the bridge, and the vertical interaction force between the vehicle and the bridge is the main force in the coupled system. The key point to establish the monorail vehicle-bridge coupled model is to precisely simulate the mechanical parameters of the rubber tyre, which has typical nonlinear characteristics. In the dynamics of tyres in a vehicle, some simplification models, such as Fiala tyre model [23], Gim tyre model [24], and Pacejka tyre model [25], were developed and applied in the dynamic analysis.

In the paper, Pacejka tyre model is considered to simulate the dynamic characteristics of the traveling wheel. In addition, the guide wheels of the suspension monorail vehicle are in direct contact with the guide tracks on the sidewalls of the track beams. When the vehicle passes through the bridge, the guide wheels interact with the track beam to provide the lateral force to the vehicle. Therefore, it is essential to build up the mutual effect between the guide wheel and track beam as well.

2.4.1. Vertical Force of Traveling Wheel. The vertical force between the traveling wheel and the track beam is defined by the relative motion trajectory between the tyre center and the deck, as shown in Figure 5. To accurately simulate the contact between the tyre and deck, the traveling wheel can be separated from the bridge deck. When the traveling wheel jumps up, the vertical force is set to be zero, which means that the vertical force of the traveling wheel can be discontinuous. Then, it can be expressed as

$$F_Z = \begin{cases} K_z\left(R_0 - R_H\right) - F_{zN} - C_z\left[v_{B_k,B_l}\right]_z & \text{for } R_H \le R_0 \\ 0 & \text{for } R_H > R_0 \end{cases}, \tag{4}$$

where K_z and C_z are the vertical stiffness and damping coefficient of the tyre, respectively; R_0 and R_H are the height of the tyre under the nominal vertical force and the height of the tyre at the moment of movement, respectively; F_{zN} is the initial nominal force of the tyre; and $[v_{B_k,B_l}]_z$ is the vertical direction of vehicle speed of the tyre center relative to the deck.

2.4.2. Longitudinal and Side Slip Force of Traveling Wheel. The lateral and longitudinal slip force of the rubber tyre of the traveling wheel can be defined according to the creep and friction coefficient under the vertical force of the tyre as

$$\begin{aligned} F_y &= -\frac{\sigma_y}{\sigma_{\text{theo}}}\frac{F_z}{F_{z_0}}\frac{\mu_y}{\mu_{y_0}}F_0\left(\sigma_{eq_y}\right), \\ F_x &= -\frac{\sigma_x}{\sigma_{\text{theo}}}\frac{F_z}{F_{z_0}}\frac{\mu_x}{\mu_{y_0}}F_0\left(\sigma_{eq_x}\right), \end{aligned} \tag{5}$$

where σ_x and σ_y represent longitudinal slip and lateral slip, respectively; $\sigma_{\text{theo}} = \sqrt{\sigma_x^2 + \sigma_y^2}$ is the theoretical tyre overall slip value; F_{z_0} and μ_{y_0} are the nominal tyre vertical force in the figure of lateral force against lateral slip and the friction coefficient at the moment, respectively; μ_x and μ_y are the friction coefficients of the longitudinal and lateral force in the current state of motion, respectively; σ_{eq_x} and σ_{eq_y} represent the friction performances of tyre in x-axis and y-axis directions, respectively.

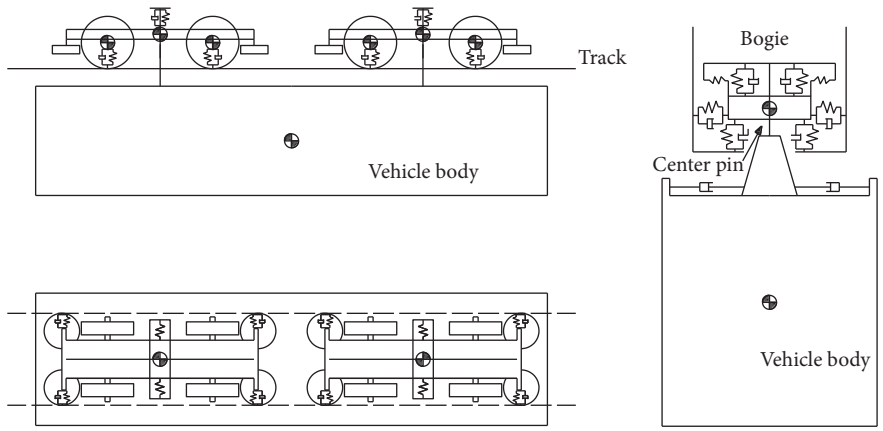

Figure 1: Dynamic model of suspension monorail vehicle.

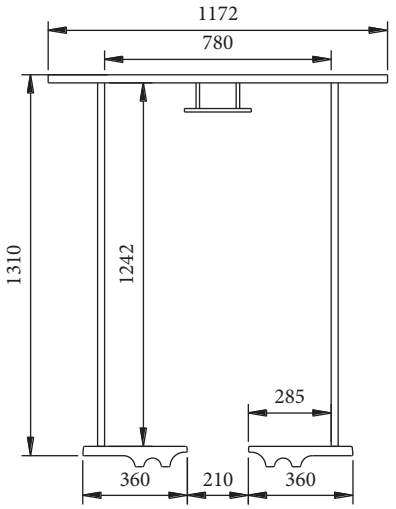

Figure 2: Cross section of the track beam end (unit: mm).

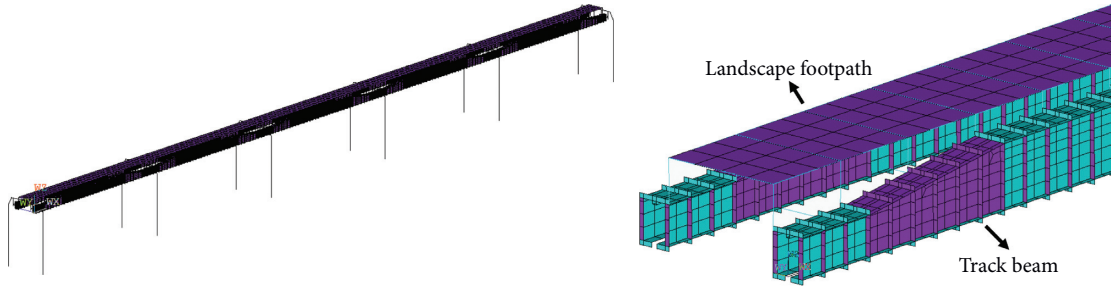

Figure 3: Finite element model of the suspension monorail system. (a) Full-bridge model. (b) Schematic diagram of the partial main beam section.

2.4.3. Lateral Force of Guide Wheel. Spring-damping force element is used to simulate the guiding force between the guide wheel and the track, which can be expressed as

$$F_{DY} = \begin{cases} K_y\left(Y_r - Y_0\right) - C_y\left[v_{D_k,D_l}\right]_y + F_{Dy\,0} & \text{for } \Delta r > 0 \\ 0 & \text{for } \Delta r \le 0 \end{cases}, \tag{6}$$

Table 1: Natural vibration characteristics of bridge structure.

Order	Frequency (Hz)	Mode shape description
1~5	0.854~0.860	Longitudinal drift of pier
6~11	0.935~1.729	Transverse bending of pier
12	3.017	Torsion of track beam
13~16	3.066~3.453	Vertical bending of track beam and footpath
17~18	3.582~3.625	Vertical bending of track beam
19	3.715	Vertical bending of track beam and footpath
20~22	4.155~4.562	Torsion of track beam

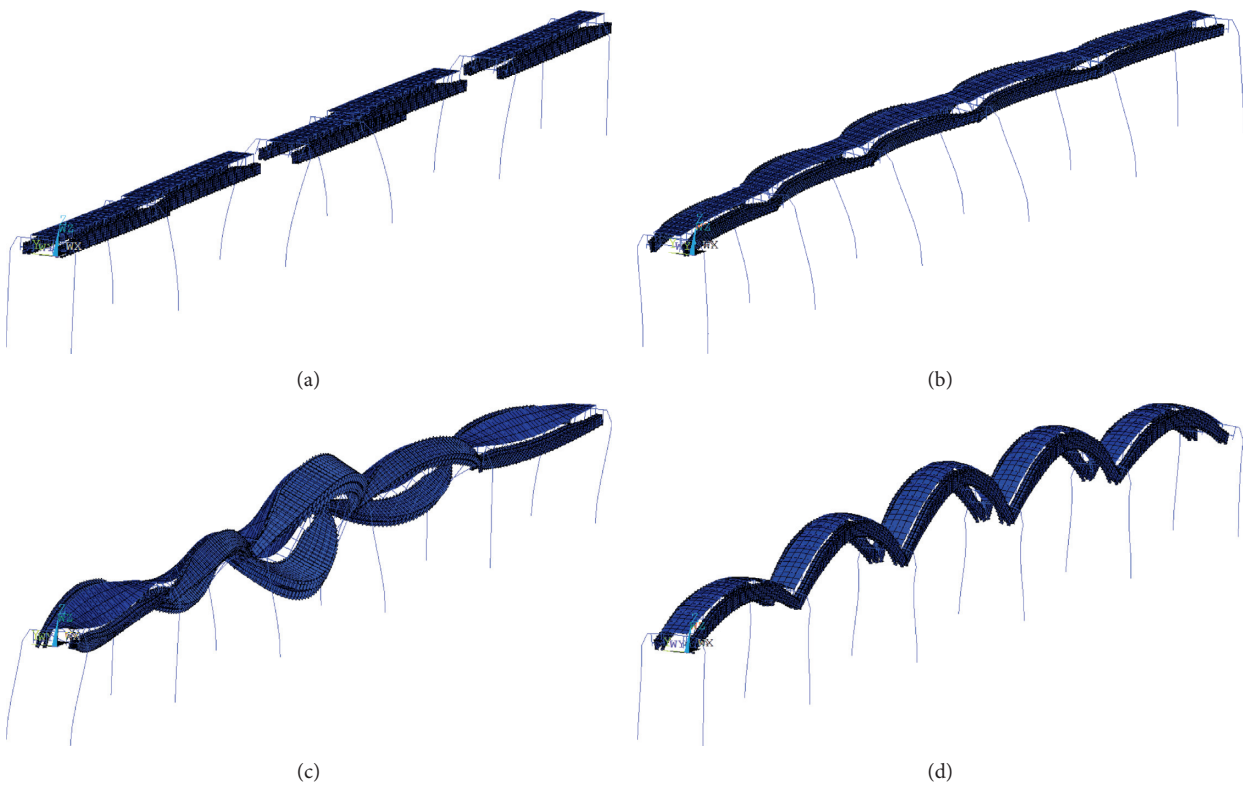

Figure 4: Typical mode shapes of the structure. (a) Longitudinal drift of pier. (b) Transverse bending of pier. (c) Torsion of track beam. (d) Vertical bending of track beam and footpath.

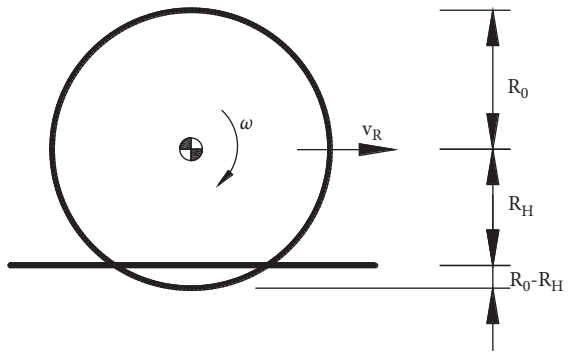

Figure 5: Schematic diagram of tyre loading deformation.

where Δr represents the radial compression of the guide wheel; K_y and C_y are the lateral stiffness and damping coefficient of the tyre, respectively; Y_r and Y_0 represent the radial compression of the guide wheel in operation state and preguiding state; F_{Dy0} represents preguiding force of the guide wheel; and $[v_{D_k,D_l}]_y$ represents the lateral component

of the speed of the guide wheel center relative to the guide track.

3. Criteria for Pedestrian Comfort on Landscape Footpath

Several countries and organizations have carried out a series of studies on the comfort of pedestrian bridges and formulated indicators and standards of comfort evaluation, such as BS 5400 [26], ISO 2631 [27] and ISO 10137 [28], CJJ69-95 [29], and EN 03 [30]. All of these standards provide the limit of the fundamental frequency, and some also propose that the structural dynamic response analysis is required if the fundamental frequency limit is not met. The limit of root mean square and peak value of accelerations are given as well. The standards of ISO and EN 03 propose the limits of both vertical and lateral accelerations, while other standards only confine the vertical acceleration.

In general, the pedestrian bridge is relatively flexible compared to other types of bridge. Its natural frequency is relatively low. The march of people may cause excessive amount of vibration on the bridge and discomfort themselves. The landscape footpath studied in the paper is different from ordinary pedestrian bridge, which is integrated with the monorail bridge. In this case, the walking people can be regarded to be scattered on the landscape footpath, as for the long span of the whole bridge system. Hence, the vibration of the landscape footpath caused by people themselves can be considered much smaller than that caused by the vehicle, which means the vehicle load dominates the dynamic responses of the bridge rather than the people load. Therefore, the paper concentrates on the study of pedestrian comfort influenced by the monorail vehicle-induced vibration; and ISO 2631 and ISO 10137 (root mean square of acceleration as the index) and EN 03 (peak value of acceleration as the index) are employed in the evaluation of the pedestrian's comfort.

3.1. Judgement by Root Mean Square of Acceleration. According to ISO 10137 and the reference curve of comfort specified in ISO 2631, for vertical acceleration, the limit of the root mean square is 60 times of the reference curve for walking people and 30 times of the reference curve for stationary people. For the lateral acceleration, the limit of the root mean square is 60 times of the reference curve. Then, the evaluation limit of RMS values of acceleration is shown in Figure 6.

3.2. Judgement by Peak Value of Acceleration. On the basis of EN 03, for the pedestrian bridges with the vertical fundamental frequency from 1.25 Hz to 2.3 Hz or second-order frequency from 2.5 Hz to 4.6 Hz and the lateral fundamental frequency from 0.5 Hz to 1.2 Hz, the peak value of acceleration is required to be examined; and the four-class evaluation standard is proposed, as shown in Table 2.

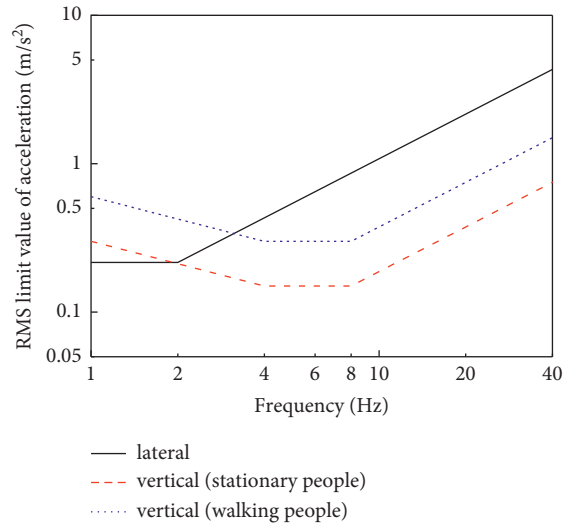

Figure 6: Evaluation limit of the root mean square value of acceleration.

Table 2: Evaluation standard of pedestrian comfort.

Comfort class	Degree of comfort	Acceleration limit (m/s²)	
		Vertical	Lateral
CL1	Maximum	<0.5	<0.1
CL2	Medium	0.5~1.0	0.1~0.3
CL3	Minimum	1.0~2.5	0.3~0.8
CL4	Unacceptable discomfort	>2.5	>0.8

4. Vehicle-Induced Dynamic Response and Judgement of Pedestrian Comfort

The dynamic response of the third span bridge in the middle of the five-span simply-supported beam is selected for analysis in the following sections. Since the bridge structure discussed in the paper is a simply supported beam, the response of midspan is larger than those of other positions. Therefore, it is reasonable to evaluate the comfort of the midspan position as a reference of the whole bridge.

4.1. Comparison of the Dynamic Response of Landscape Footpath and Track Beam. In this section, the speed of the vehicle is selected as 60 km/h, and the lateral and vertical displacements in the midspan of the landscape footpath and track beam are shown in Figure 7.

According to Figure 7, it can be seen that the response of the landscape footpath is different from that of the track beam. The displacements of the landscape footpath and track beam basically coincide when the vehicle has not driven into or exited the span. The displacement is mainly delivered by the bridge pier, which is acted by other spans.

It can be seen from Figure 7(a) that the lateral displacement of the track beam is obviously shifted to the

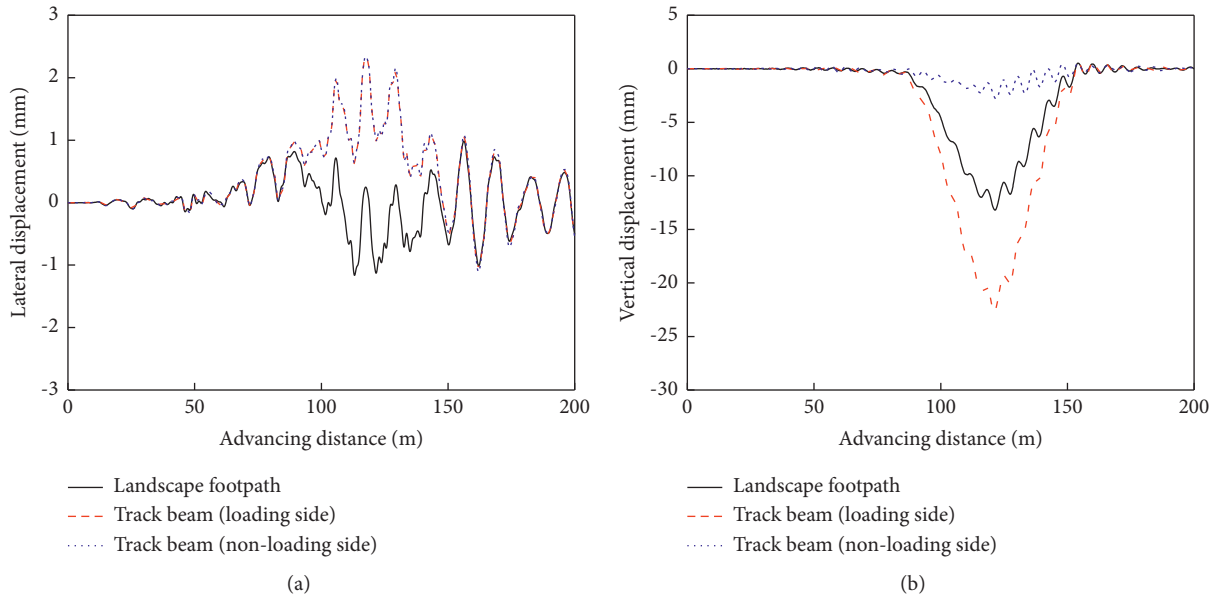

Figure 7: Comparison on time history of midspan displacements of landscape footpath and track beam. (a) Lateral. (b) Vertical.

loading side, and the lateral displacements of the two track beams are the same. It is simply due to the fact that the vibration on the load side is transferred to the other side via the pier. On the other hand, the landscape footpath vibrates at its equilibrium position in the lateral direction. The landscape footpath is paved on the track beam through the structure components. The responses of the landscape footpath are weakened to a certain extent when the vibration transmits from the track beam to the footpath. It is supposed that the structure components between the track beam and footpath have a certain amount of displacement and rotation. The maximum lateral displacement of the track beam is 2.34 mm, while the maximum value of the landscape footpath is only 1.16 mm.

As for the vertical displacement in Figure 7(b), when the vehicle enters the objective span section, the eccentric load of the vehicle would affect the dynamic response. The maximum vertical displacement of the track beam is 22.6 mm. The maximum value of the landscape footpath is only 13.2 mm, which is only 58.4% of the value of the track beam.

The comparison between the lateral and vertical accelerations in the midspan of the landscape footpath and track beam is shown in Figure 8.

The lateral and vertical displacements of the track beam applied to the load are greater than those of the landscape footpath, due to the fact that the track beam directly bears the vehicle load. The peak values of the lateral and vertical acceleration of the track beam (loading side) are 0.459 m/s^2 and 0.639 m/s^2, respectively. The peak values of the lateral and vertical acceleration of the landscape footpath are 0.353 m/s^2 and 0.456 m/s^2, respectively, which are 30.0% and 40.1% larger than those of the track beam, respectively.

4.2. Dynamic Response Analysis of Landscape Footpath. The lateral and vertical displacements in the midspan of the landscape footpath at different vehicle speeds are shown in Figure 9.

It can be seen from the figure that the bridge pier will be induced to vibrate by the load applied to the adjacent beam before the vehicle enters the objective span. It results in a large lateral displacement in the midspan and a negligible vertical displacement. The peak value of the lateral displacement of the landscape footpath appears at a speed of 30 km/h; and there are two moments where relatively large displacements occur during the time in which the vehicle passes the bridge. The vertical displacement enhances with the increase of the vehicle speed. When the speed of the vehicle is 60 km/h, the vertical vibration appears during the monorail vehicle passes through the bridge.

The lateral and vertical accelerations in the midspan of the landscape footpath at different vehicle speeds are shown in Figure 10.

From Figures 10(a) and 10(b), the lateral acceleration reaches peak when the vehicle's speed is 40 km/h, while vertical acceleration reaches peak when the speed is 50 km/h. The lateral and vertical accelerations are comparatively large when the speed is over 40 km/h. The lateral acceleration is large when the vehicle passes on the bridge. The characteristics of vertical vibration are different from those of lateral vibration. When the vehicle's speed is 50 km/h, the vertical vibration of the landscape footpath markedly intensifies when the vehicle exits the span. When the vehicle's speed is 60 km/h, the landscape footpath vibrates obviously during the time in which the monorail vehicle is passing through.

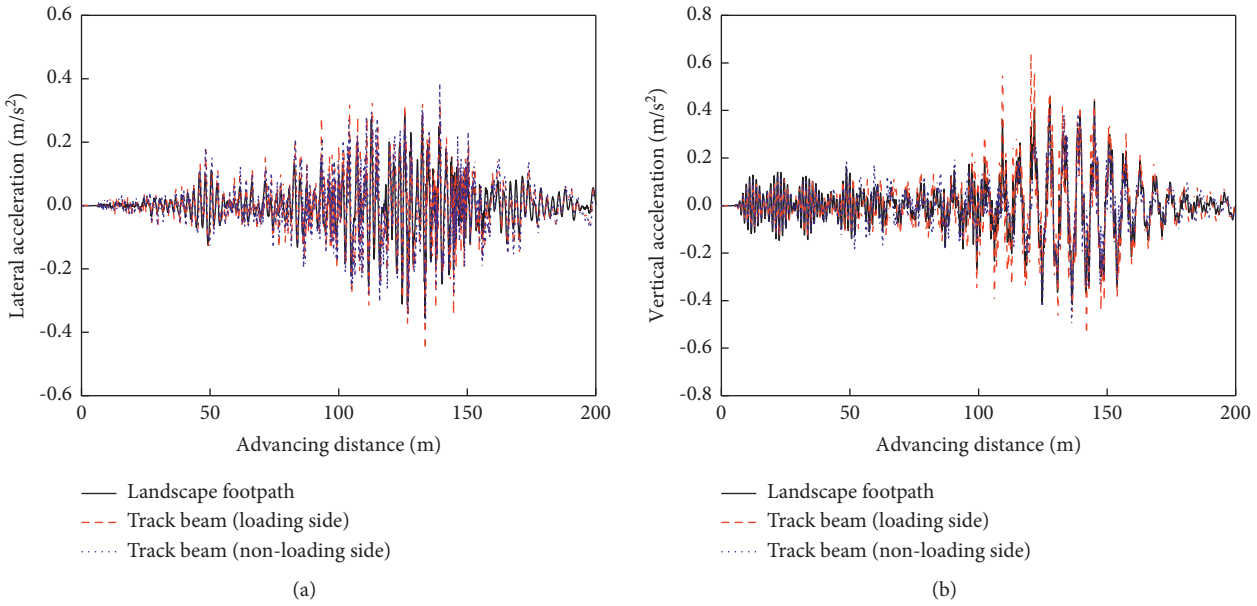

Figure 8: Comparison on time history of midspan accelerations of landscape footpath and track beam. (a) Lateral. (b) Vertical.

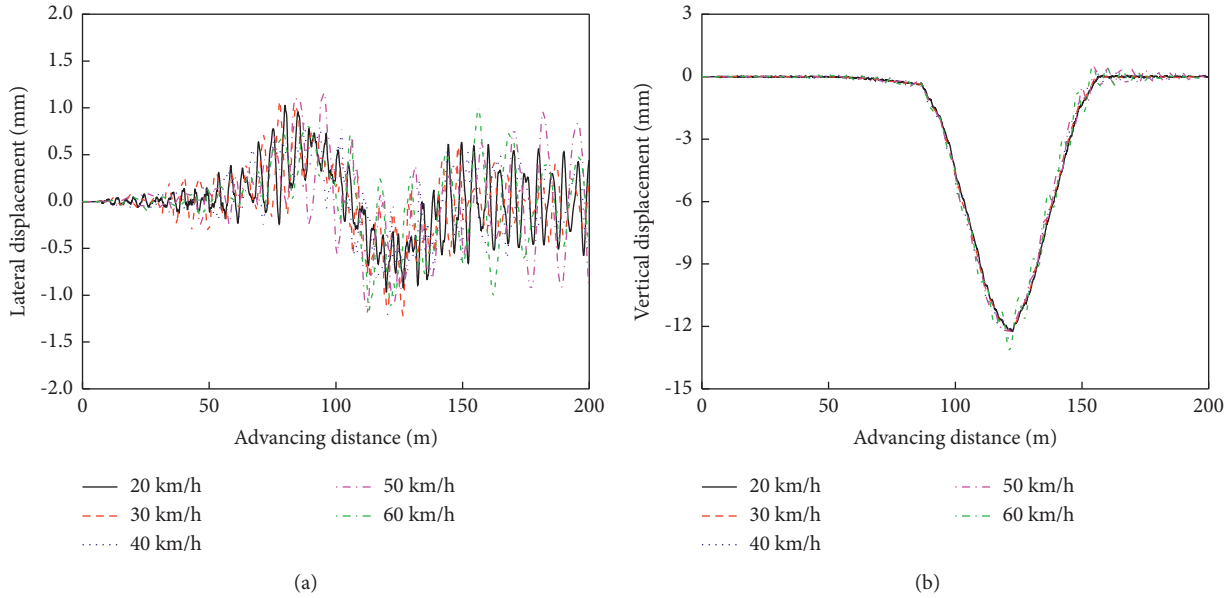

Figure 9: Comparison on time history of midspan displacements of landscape footpath at different vehicle speeds. (a) Lateral. (b) Vertical.

4.3. Evaluation of the Pedestrian's Comfort. By analyzing the time history of the acceleration in Figure 9, the RMS and peak values of the acceleration can be obtained; and the time histories of the acceleration during the time in which the vehicle passes the bridge can be extracted in Table 3.

Based on the RMS value evaluation of the standard ISO 10137, the maximum values of the lateral and vertical acceleration are 0.162 m/s^2 and 0.169 m/s^2, respectively, which meet the requirement. According to the peak value evaluation of the standard EN 03, the maximum lateral acceleration is 0.546 m/s^2 which satisfies CL3 standard, while the maximum vertical acceleration is 0.548 m/s^2 which meets CL2 standard.

On the whole, the pedestrian comfort of the landscape footpath paved on the suspension monorail beam meets the relevant requirements, and the lateral comfort is slightly worse than the vertical comfort.

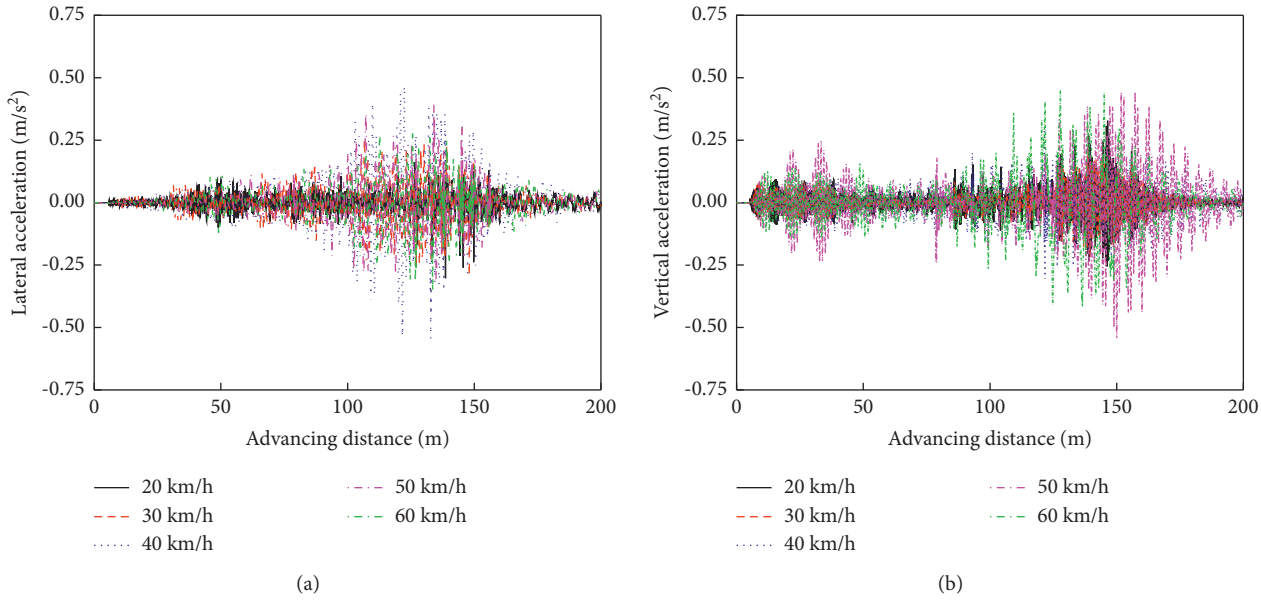

Figure 10: Comparison on time history of midspan accelerations of landscape footpath at different vehicle speeds. (a) Lateral. (b) Vertical.

Table 3: Midspan acceleration values of landscape footpath at different vehicle speeds.

Acceleration		Vehicle speed				
		20 km/h	30 km/h	40 km/h	50 km/h	60 km/h
RMS value (m/s^2)	Lateral	0.041	0.093	0.162	0.121	0.105
	Vertical	0.067	0.057	0.084	0.144	0.169
Peak value (m/s^2)	Lateral	0.302	0.297	0.546	0.392	0.353
	Vertical	0.328	0.229	0.306	0.548	0.456

5. Conclusions

Under the background of the first practical application of the landscape footpath paved on the suspension monorail system, the paper analyzes the dynamic responses of track beam and landscape footpath of the suspension monorail at different vehicle speeds by establishing the monorail vehicle-bridge coupled system. The pedestrian comfort level on the landscape footpath during the time in which the vehicle is passing the bridge is evaluated. The main conclusions are as follows:

(1) The dynamic response of the landscape footpath is obviously different from that of the track beam. For the lateral displacement, due to the displacement and rotation of the structure components which support the landscape footpath, the lateral vibration transmitted to the footpath is weakened.

(2) The lateral and vertical displacements of the loaded track beam are greater than that of the landscape footpath; and the maximum acceleration of the track beam is about 1.3 to 1.4 times that of the landscape footpath.

(3) The vertical displacement generally augments with the increase of the vehicle speed. However, when the vehicle's speed is 50 km/h, the vertical acceleration of the bridge markedly intensifies when the vehicle exits the span.

(4) The root mean square (ISO 10137) and peak value (EN 03) of acceleration are chosen to evaluate the pedestrian comfort.

Data Availability

The data generated or analyzed during this study are included within this article.

Conflicts of Interest

The authors declare that they have no conflicts of interest.

Acknowledgments

This work was supported in part by a grant from China Construction Science and Industry Corp., Ltd., and China Railway Eryuan Engineering Group Co., Ltd.

References

[1] Mohurd, *Code for Design of Urban Rail Transit Bridge. GB/T 51234-2017*, China Architecture and Building Press, Beijing, 2017.

[2] Housing and Urban-Rural Development Department of Henan Province, *Technical Standard for Suspension Monorail Transit*, Housing and Urban-Rural Development Department of Henan Province, Zhengzhou, 2019.

[3] Y. Bao, Y. Li, and J. Ding, "A case study of dynamic response analysis and safety assessment for a suspended monorail system," *International Journal of Environmental Research and Public Health*, vol. 13, no. 11, p. 1121, 2016.

[4] Y.-l. Bao, H.-y. Xiang, Y.-l. Li, C.-j. Yu, and Y.-c. Wang, "Study of wind-vehicle-bridge system of suspended monorail during the meeting of two trains," *Advances in Structural Engineering*, vol. 22, no. 8, pp. 1988–1997, 2019.

[5] Q. L. He, C. B. Cai, S. Y. Zhu, J. W. Zhang, and W. M. Zhai, "Field measurement of the dynamic responses of a suspended monorail train–bridge system," *Proceedings of the Institution of Mechanical Engineers - Part F: Journal of Rail and Rapid Transit*, vol. 234, no. 10, Article ID 095440971988073, 2019.

[6] Y. Yang, Q. He, C. Cai, S. Zhu, and W. Zhai, "Coupled vibration analysis of suspended monorail train and curved bridge considering nonlinear wheel-track contact relation," *Vehicle System Dynamics*, pp. 1–28, 2021.

[7] Y. Zou, Z. Liu, K. Shi et al., "Experimental study of aerodynamic interference effects for a suspended monorail vehicle-bridge system using a wireless acquisition system," *Sensors*, vol. 21, no. 17, p. 5841, 2021.

[8] P. Feng, Z. Wang, F. Jin, and S. Zhu, "Vibration serviceability assessment of pedestrian bridges based on comfort level," *Journal of Performance of Constructed Facilities*, vol. 33, no. 5, Article ID 04019046, 2019.

[9] D. Y. Chen, S. P. Huang, and Z. Y. Wang, "A theory of pedestrian-induced footbridge vibration comfortability based on sensitivity model," *Advances in Bridge Engineering*, vol. 24, no. 2, 2021.

[10] R. Ma, L. Ke, D. Wang, A. Chen, and Z. Pan, "Experimental study on pedestrians' perception of human-induced vibrations of footbridges," *International Journal of Structural Stability and Dynamics*, vol. 18, no. 10, Article ID 1850116, 2018.

[11] B. Bhowmik, B. Hazra, M. O'Byrne, B. Ghosh, and V. Pakrashi, "Damping estimation of a pedestrian footbridge - an enhanced frequency-domain automated approach," *Journal of Vibroengineering*, vol. 23, no. 5, pp. 14–25, 2021.

[12] B. Chen, D. Wu, X. Xie, and P. Lu, "Comfort assessment for a pedestrian passageway suspended under a girder bridge with random traffic flows," *Advances in Structural Engineering*, vol. 20, no. 2, pp. 225–234, 2017.

[13] C. J. Cui, R. J. Ma, X. H. Hu, and W. C. He, "Vibration analysis for pendent pedestrian path of a long-span extradosed bridge," *Sustainability*, vol. 11, no. 17, p. 4664, 2020.

[14] W. M. Zhai, S. L. Wang, N. Zhang, M. M. Gao, and C. F. Zhao, "High-speed train-track-bridge dynamic interactions - part II: experimental validation and engineering application," *International Journal of Reality Therapy*, vol. 1, no. 1-2, pp. 25–41, 2013.

[15] T. Arvidsson and R. Karoumi, "Train-bridge interaction - a review and discussion of key model parameters," *International Journal of Reality Therapy*, vol. 2, no. 3, pp. 147–186, 2014.

[16] Y. Li, X. Xu, Y. Zhou, C. Cai, and J. Qin, "An interactive method for the analysis of the simulation of vehicle-bridge coupling vibration using ANSYS and SIMPACK," *Proceedings of the Institution of Mechanical Engineers - Part F: Journal of Rail and Rapid Transit*, vol. 232, no. 3, pp. 663–679, 2018.

[17] H. Xiang, P. Tang, Y. Zhang, and Y. Li, "Random dynamic analysis of vertical train-bridge systems under small probability by surrogate model and subset simulation with splitting," *Railway Engineering Science*, vol. 28, no. 3, pp. 305–315, 2020.

[18] Y. Bao, W. Zhai, C. Cai, X. Yuan, and Y. Li, "Impact coefficient analysis of track beams due to moving suspended monorail vehicles," *Vehicle System Dynamics*, pp. 1–17, 2020.

[19] Q. He, C. Cai, S. Zhu, K. Wang, and W. Zhai, "An improved dynamic model of suspended monorail train-bridge system considering a tyre model with patch contact," *Mechanical Systems and Signal Processing*, vol. 144, Article ID 106865, 2020.

[20] Y. Bao, W. Zhai, C. Cai, S. Zhu, and Y. Li, "Dynamic interaction analysis of suspended monorail vehicle and bridge subject to crosswinds," *Mechanical Systems and Signal Processing*, vol. 156, no. 2, Article ID 107707, 2021.

[21] S. Dietz, G. Hippmann, and G. Schupp, "Interaction of vehicles and flexible tracks by co-simulation of multibody vehicle systems and finite element track models," *Vehicle System Dynamics*, vol. 37, no. S1, pp. 372–384, 2002.

[22] M. Rose, R. Keimer, and E. J. Breitbach, "Parallel robots with adaptronic components," *Journal of Intelligent Material Systems and Structures*, vol. 15, no. 9-10, pp. 763–769, 2004.

[23] E. Fiala, "Seitenkrafte am rollenden luftreifen," *VDI-Zeitschrift*, vol. 96, p. 973, 1954.

[24] G. Gim, Y. Choi, and S. Kim, "A semiphysical tyre model for vehicle dynamics analysis of handling and braking," *Vehicle System Dynamics*, vol. 43, no. S1, pp. 267–280, 2005.

[25] H. B. Pacejka, *Tire and Vehicle Dynamics*, Butterworth-Heinemann, UK, Third Edition, 2012.

[26] Bsi, *Steel concrete and Composite Bridges Part 2: Specification for Loads*, British Standard Institute, London, 2006.

[27] Iso, *Mechanical Vibration and Shock - Evaluation of Human Exposure to Whole-Body Vibration Part 4: Guidelines for the Evaluation of the Effects*, International Organization for Standardization, Switzerland, 2010.

[28] Iso, *Bases for Design of Structures - Serviceability of Buildings and Walkways against Vibrations*, International Organization for Standardization, Switzerland, 2007.

[29] Institute of Standard and Quota of Ministry of Construction, *Technical Specifications for Urban Pedestrian Overcrossing and Underpass*, Institute of standard and quota of Ministry of construction, Beijing, 1996.

[30] Directorate-General for Research and Innovation, *Human-induced Vibrations of Steel Structures - Design of Footbridges Guidelines. Footbridge Guidelines EN 03*, Publications Office of the European Union, Luxembourg, 2010.